

## Collaborational Effect of Layered Configuration for Enhancement of Microwave Heating

**Masato M. Maitani,<sup>\*a</sup> Tomoharu Inoue,<sup>a</sup> Yohei Tsukushi,<sup>a</sup> Niklas D. J. Hansen,<sup>b</sup> Dai Mochizuki,<sup>a</sup> Eiichi Suzuki,<sup>a</sup> Yuji Wada<sup>\*a</sup>**

<sup>a</sup>Department of Applied Chemistry, Graduate School of Science and Engineering, Tokyo Institute of Technology, 2-12-1 Ookayama, Meguro, Tokyo 152-8552, Japan.

<sup>b</sup>School of Information and Communication Technology, Royal Institute of Technology, Electrum 229, 164 40, Kista, Sweden.

E-mail: mmaitani@apc.titech.ac.jp(MMM), yuji-w@apc.titech.ac.jp (YW).

Phone/fax: +81-5734-2879.

### S1. Temperature-Radiation Relation of Each Material

Since each material has different infrared emissivity detected by an IR thermographic camera at a certain temperature, we measured a standard curve of sample temperature as a function of observed temperature by IR thermographic camera for each sample, bare quartz glass, bare FTO, bare Ti, and  $\text{TiO}_2/\text{FTO}$ . Each sample was partially coated by a quasi-blackbody paint (JCS-3, emissivity: 0.94(0~1500 °C), Japan Sensor, co.) and heated by a hotplate in ambient and the same IR thermographic camera was used to detect the temperature at blackbody coating and sample surface to earn the calibration curve correlating between the real sample temperature measured on blackbody coating and observed temperature on the sample surfaces. All of temperature data was calibrated based on this temperature-radiation relation in the main section by applying the fitting parameters in Table S1.

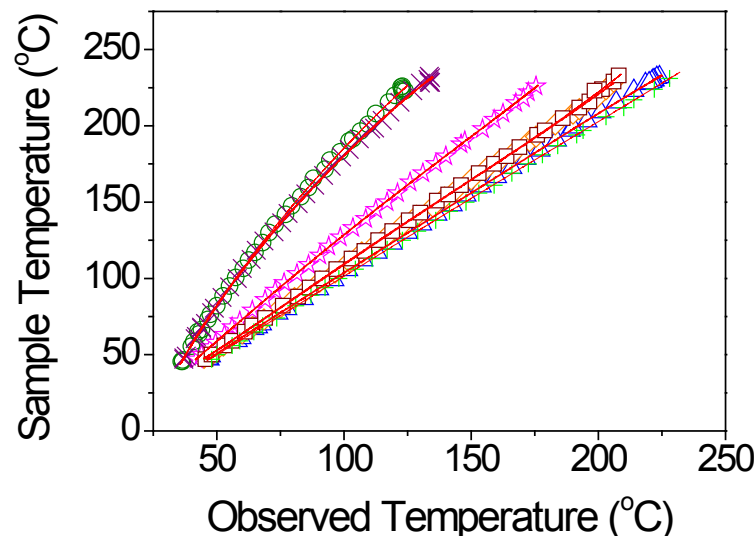


**Figure S1** Standard curves of observed temperature as a function of sample temperature with  $\text{TiO}_2/\text{FTO}$ (diamond),  $\text{TiO}_2/\text{FTO}$  annealed(star),  $\text{TiO}_2/\text{SiO}_2$ (+),  $\text{TiO}_2/\text{Ti}$ (square), bare FTO(circle), bare  $\text{SnO}_2$ (triangle), and bare Ti(X).

**Table S1** The polynomial fitting parameters,  $y=ax^4+bx^3+cx^2+dx+e$ , of standard curves in Fig. S1.

Sample	a	b	c	d	e
$\text{TiO}_2/\text{FTO}$ ann <sup>a</sup>	6.91768E-08	- 2.62577E-05	2.48819E-03	1.35152E+00	- 1.21493E+01
$\text{TiO}_2/\text{FTO}$	7.19337E-08	- 3.37971E-05	5.49133E-03	7.57383E-01	5.00301E+00
$\text{TiO}_2/\text{Ti}$	8.73212E-08	- 3.85062E-05	5.73646E-03	7.89914E-01	3.17717E+00
$\text{TiO}_2/\text{SnO}_2$	1.11790E-08	- 6.07128E-06	1.04099E-03	9.58509E-01	1.14294E-01
Bare Ti	-7.03076E-07	2.78907E-04	- 4.58399E-02	5.27652E+00	- 9.74888E+01
Bare FTO	-3.24513E-07	1.43290E-04	- 2.81029E-02	4.38164E+00	- 8.25852E+01
Bare $\text{SiO}_2$	-2.47387E-08	1.28657E-05	2.43692E-03	1.24532E+00	- 6.83648E+00

<sup>a</sup> Sample is after annealed in a electric oven at 500 °C for 30min in ambient.

## S2. Angle Dependence of $\text{TiO}_2/\text{FTO}$ on Temperature Increase

To acquire further information of MW heating of  $\text{TiO}_2/\text{FTO}$ , the tilt angle dependence of sample in terms of the oscillating electric field in SM-MW cavity on the temperature increase was also measured in Figure S2. The efficiency of the MW heating revealed inert by tilting the sample in psi angle (indicated in inset). The initial temperature of  $\text{TiO}_2/\text{FTO}$  and bare FTO appeared differently due to the inaccuracy of the standard curves of observed temperature as a function of sample temperature in the room temperature region, although all of sample was heated in ambient.

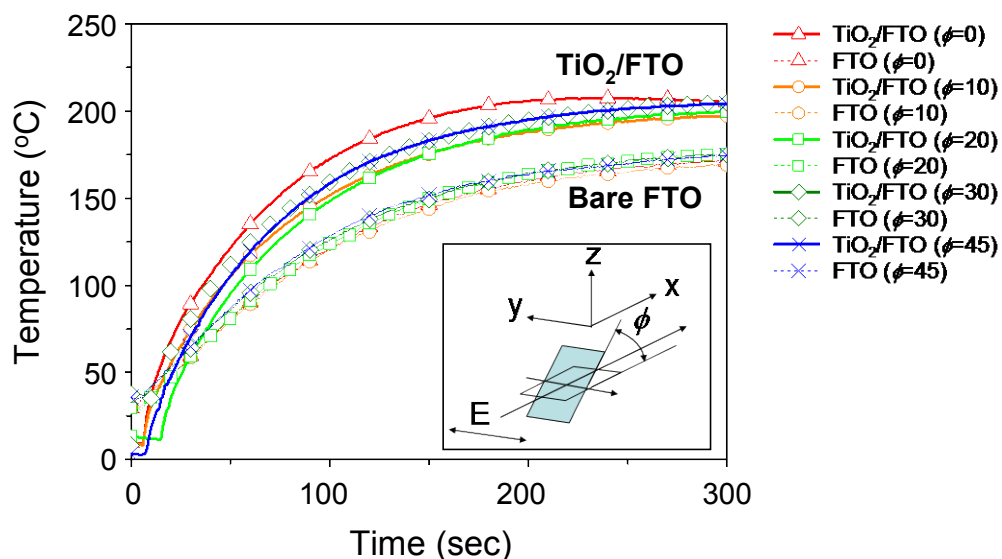


**Figure S2** Dependence of sample tilt angle,  $\phi$ , on the averaged temperature in the sampled area of  $\text{TiO}_2$  on FTO and bare FTO measured by IR thermographic camera with calibration of temperature-radiation relation.

### S3. Temperature Increase of TiO<sub>2</sub>/FTO under Magnetic Field

The temperature changes of TiO<sub>2</sub>/FTO and bare FTO were measured by an IR thermographic camera with calibration of temperature-radiation relation under MW irradiation at the node of electric field, where the magnetic field reveals maximum, with the MW power of 5.8 W in an SM-MW cavity in Figure S3. The temperature increase of both TiO<sub>2</sub>/FTO and FTO revealed much less efficiency and deference in temperature of about ~20 °C.

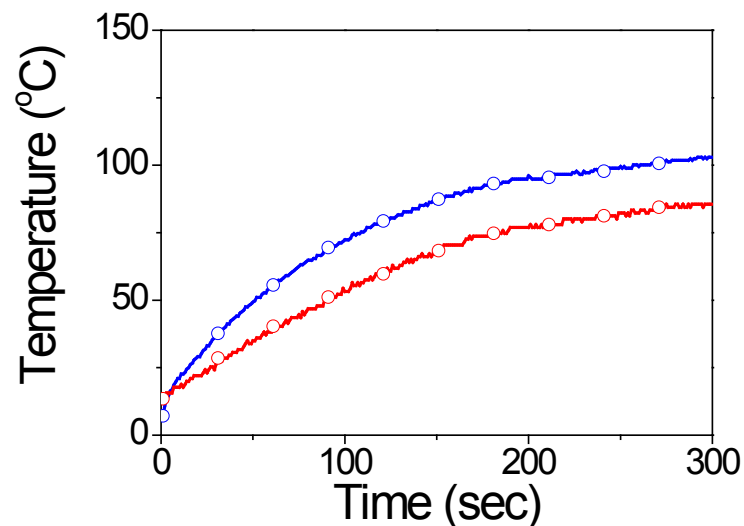


**Figure S3** The averaged temperature in the sampled area of TiO<sub>2</sub>/FTO (red) and FTO (blue) located at the node of electric field measured by an IR thermographic camera with calibration of temperature-radiation relation under MW irradiation with power of 5.8 W.

#### S4. Temperature Increase of Oxide Porous Films on FTO

To generalize the results of  $\text{TiO}_2$  on FTO, MW heating is applied to several different kinds of oxide porous film on FTO substrates. The films are prepared by the same procedures as  $\text{TiO}_2$  films, while the pastes (10wt%) of oxides particles were made of commercially available particular samples of  $\text{Nb}_2\text{O}_5$  (99.9%, 144-05332, Wako),  $\text{MnO}_2$  (<5 $\mu\text{m}$ , 217646-100G, Aldrich),  $\text{Bi}_2\text{O}_3$  (99.9%, 028-08842, Wako),  $\text{Ta}_2\text{O}_5$  (200-09342, 99.9%, Wako), and  $\text{SnO}_2$  (<100nm, 549657-5G, Aldrich) grained with ethanol and ethyl cellulose in a bowl mill. These pastes were coated on FTO and quartz glass substrates by the doctor blade method followed by a pre-annealing at 130 °C on a hot plate for 6 min for leveling resulting in a few micron thick films on substrates. The sample films on FTO or quartz glass were then loaded into the SM-MW cavity possessing the maximum electric field and temperature increase was also measured in Figure S4. The temperature of most of oxide films on FTO increased more efficiently than FTO without films and same oxide films on quartz substrates. The negligible temperature increase with only the oxide films proved that the oxide films itself is MW-inert, which are unable to absorb MW at 2.45GHz. As applied to  $\text{TiO}_2$  films in S1, the calibration of IR thermographic camera was also applied to each oxide film on FTO or quartz glass substrates by measuring the standard curve with coating samples by a quasi-blackbody paint, while the calibration curve is not exhibited.

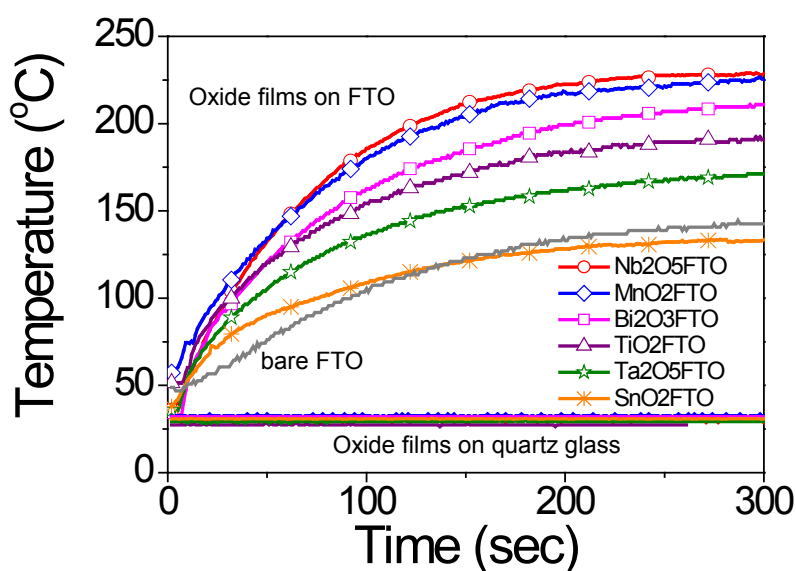


**Figure S4** Mean temperature in the sampled area measured by IR camera of each oxide films on FTO and on quartz glass substrates under MW irradiation (5W) with calibration of temperature-radiation relation.

### S5. Annealing Temperature of TiO<sub>2</sub>/FTO for DSSC

The annealing temperature of TiO<sub>2</sub>/FTO was measured by an IR thermographic camera in an SM-MW cavity with the calibration of temperature-radiation relation in Figure S5. The annealed TiO<sub>2</sub>/FTO was used to the DSSC application in the main section.

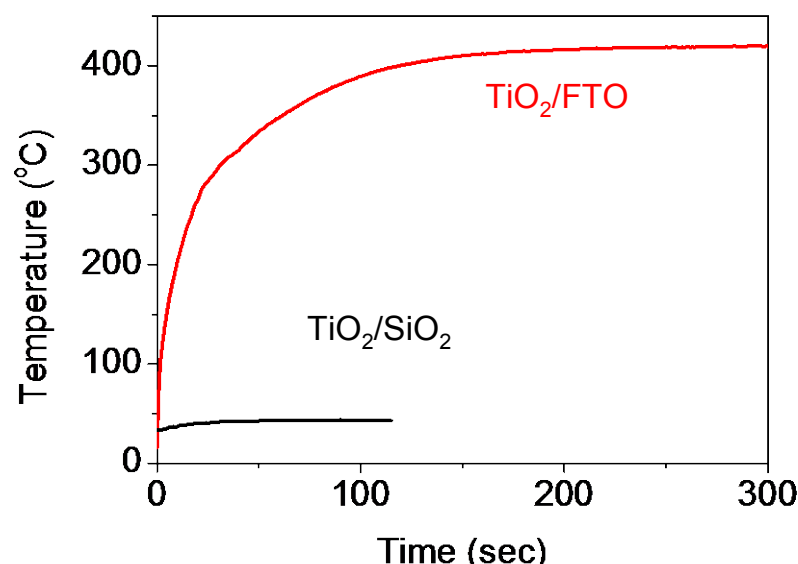


**Figure S5** The averaged temperature in the sampled area of TiO<sub>2</sub> on FTO and bare FTO measured by an IR thermographic camera with calibration of temperature-radiation relation under MW irradiation with power of 39W. As reference, the temperature change of the same TiO<sub>2</sub> film on SiO<sub>2</sub> glass was measured in the same MW annealing setup and revealed almost inert for MW heating.

## S6. Experimental Details

### *Film Preparations:*

A commercially available  $\text{TiO}_2$  paste (PST-18NR, JGC Catalysts and Chemicals Ltd.) was applied on to the substrates, FTO, Ti, and  $\text{SiO}_2$  (W1 x D2cm) to prepare 10 micrometer thick uniform  $\text{TiO}_2$  film by the doctor blade method. All samples were pre-annealed at 130 °C on a hot plate for 6 min for levelling. The samples were annealed either in SM-MW cavity (2.5 or 5 min) or conventional electric oven (30 min).

### *MW Annealing:*

MW cavity was built for  $\text{TE}_{103}$  single mode connected to 2.45 GHz semiconductor generator (Fuji Electronic Industrial Co., Ltd.). The resonance of  $\text{TE}_{103}$  mode was tuned after placing samples by a three stub and a plunger under MW irradiation of 1W prior to each experiment in order to minimize the reflected power from the cavity (< 0.1W). The surface temperature of samples was measured by a CCD infrared thermographic camera (ARTCAM-320THERMO-WOM-TMC, Artray Co., Ltd.) and averaged with nine spots on samples as the mean temperature. The real temperature was calculated from the measured temperature with radiation-temperature dependence calibrated by a controlled measurement of same samples(S1).

### *Solar Cell Assembly and Evaluation:*

Annealed samples (S5) were immersed in an ethanolic solution of Ru dye-sensitizer, N719 (Solaronix), for 12h and rinsed by ethanol. The dye-sensitized  $\text{TiO}_2$ /FTO was then assembled in a sandwich cell configuration with iodine electrolyte (0.1M LiI, 0.6 M 1-butyl-3-methyl-imethylimidazolium iodide, 0.03 M  $\text{I}_2$ , and 0.5 M 4-*tert*-butylpyridine in 15/85 (v/v) mixture of valeronitrile and acetonitrile), platinum counter electrode, and 70  $\mu\text{m}$  thick Surlyn (DuPont) providing 0.4x0.4 cm<sup>2</sup> as the active cell area. The photocurrent-voltage properties of solar cells were evaluated under AM1.5 solar simulator (YY5-100, Yamashita Denso).

### *Sample Configurations:*

The sample configurations of each  $\text{TiO}_2$  films, FTO, Ti, quartz glass were indicated as follows. The thickness of each sample was measured by either cross-section SEM or scanning probe microscope.

$\text{TiO}_2$  film: 10um thick after pre-annealed on a hot plate.

$\text{TiO}_2$  film after annealing: 4  $\mu\text{m}$  thick after annealed in a electric oven for 30min at 500 °C.

Ti: 100 nm thick Ti metal was deposited on a glass substrate (1mm thick) under high vacuum in a thermal deposition chamber.

Quartz ( $\text{SiO}_2$ ) glass: 1 mm thick glass as purchased.

FTO: 1  $\mu\text{m}$  thick F: $\text{SnO}_2$  on glass (1mm) as purchased from Nihon Shield Glass, Japan.